Mathematical Modeling to Evaluate the Accuracy of Computer Vision for the Near-Zero Motion Detection of Astronomical Objects

Sergii Khlamov, Vadym Savanevych, Iryna Tabakova, Tetiana Trunova and Ihor Levykin

Kharkiv National University of Radio Electronics, Nauki avenue 14, Kharkiv, 61166, Ukraine

Abstract

In this paper we developed a method for the mathematical modeling for the near-zero apparent motion (NZAM) detection of astronomical objects in series of CCD-frames using the methods of statistical and in situ modeling. Such method helps to evaluate the accuracy of computer vision in scope of the NZAM detection of astronomical objects. We have described all especial variables and preconditions for the methods of statistical and in situ modeling. The method with a maximum likelihood criterion and the method with the Fisher distribution were selected as specific algorithms for a NZAM detection of astronomical objects in scope of the research. A method for the mathematical modeling for a NZAM of objects of objects in a series of CCD-frames was developed using the C++ programming language. The modeling results were analyzed using the especial quality indicator, like a conditional probability of true detection, so the selected detection algorithms were evaluated using both statistical and in situ imitation modeling techniques.

Keywords

Statistical modeling, imitation modeling, in situ modeling, computer vision, OLS-evaluation, F-test, maximum likelihood criterion, near-zero motion detection, series of images

1. Introduction

Nowadays the modern algorithms for a series of images processing should save the balance between speed and quality of processing of such huge amount of information, which is produced by data streams from the different sources. To proof the high quality of the object's detection, such algorithms should be tested not only in the real situation, but also in the virtual simulation using the predefined dataset. This can be achieved using the statistical imitation [1, 2] or in situ modeling [3] when the detection algorithm is developed. Because the sooner we test the algorithm and find inaccuracies in it, the faster we can release it without bugs. This is the main goal of all software development lifecycles.

The modern detection algorithms should detect and recognize objects with the different apparent motion: zero motion (fixed object), near-zero motion, normal motion, high-speed motion, etc. There is no one unified algorithm, which can detect and recognize all objects with motion in all described above cases. So, in our paper we focused on the detection algorithms for the objects that have a near-zero apparent motion (NZAM).

The object, which has a NZAM is the kind of objects, which has a very small shift in pixels between frames at the moment of capturing. And this shift is commensurate with the measuring error of its position. Such object has a velocity between frames in series that is less than or equal to 3 root mean square (RMS) errors (3σ) of measurements of their positions [4]. There are different types of

COLINS-2023: 7th International Conference on Computational Linguistics and Intelligent Systems, April 20–21, 2023, Kharkiv, Ukraine
EMAIL: sergii.khlamov@gmail.com (S. Khlamov); vadym.savanevych1@nure.ua (V. Savanevych); iryna.tabakova@nure.ua (I. Tabakova); tetiana.trunova@nure.ua (T. Trunova); ihor.levykin@nure.ua (I. Levykin)
ORCID: 0000-0001-9434-1081 (S. Khlamov); 0000-0001-8840-8278 (V. Savanevych); 0000-0001-6629-4927 (I. Tabakova); 0000-0003-2689-2679 (T. Trunova); 0000-0001-8086-237X (I. Levykin)

moving objects with a NZAM in the series of frames. Such types of moving objects are drones [5], robots [6, 7], satellites [8], rockets, and even asteroids [9]. So, these moving objects are objects that can be shotted by the CCD-camera [10] and the motion of which should be detected. The NZAM of objects is presented because of the various observational conditions: CCD-matrix resolution, exposure time, object direction, which is perpendicular to the shotting point, very big distance to the object or even extremely slow apparent motion of the destination object.

The main point to detect the object in an image is to recognize it after image filtering [11] and determine the parameters of the object's image [12, 13, 14] and trajectory [4]. A goal of the modern algorithms and software [15, 16, 17] is to speed up as much as possible the processing of such input series of images/CCD-frames to recognize objects and process the information from its image in scope of the machine vision [18]. In general, the modern algorithms for detection of the astronomical objects are based on checking the hypotheses H_0 (object has no apparent motion in the image plane) and H_1 (object has up to 3σ-velocity or even more) [19]. The main detection principle is based on using the following specific quality indicators: conditional probabilities of the false detection (CPFD) and conditional probability of true detection (CPTD) [20]. In this paper we showed a several detection algorithms that use both the maximum likelihood criterion [21] and the Fisher f-criterion [22] to test the developed methods of statistical and in situ modeling for the object's NZAM detection in series of images.

The purpose of this paper is to develop a method for the mathematical modeling for the NZAM detection of astronomical objects in series of frames using the methods of statistical and in situ modeling. Such method will help to evaluate the accuracy of computer vision in scope of the NZAM detection.

2. Detection algorithms

2.1. Maximum likelihood criterion

In general, the hypothesis H_0 and alternative hypothesis H_1 are verified by the maximum likelihood criterion [23] or other criterion from the statistical checking group called Bayesian [24]. In this case, the likelihood ratio will be like a final value of statistic for the appropriate criteria. Such value in the common case assimilates with the predefined critical values (calculated or even from the table) [25].

There are several various situations for the maximum likelihood ratio. Almost all of them depend on the knowledge of the variance σ^2 of the object's position.

So, in general, the following variations of the substitutional methods for the maximum likelihood detection of a NZAM can be used:

- variance σ^2 of the object's position is known;
- variance σ^2 of the object's position is unknown and only the estimation of such variance σ^2_{est} can be used;
- external variance estimation σ^2_{out} of the object's position can be used based on the previous calculations according to the accuracy of previous measurements sets (for example, the already known instrumental error during observation).

In some case it can be known, otherwise the external estimation of the variance σ^2 of object's position is used for this purpose. Such external estimation in the common case is calculated from the estimation accuracy from the previous array of positional measurements.

The method for the object's NZAM detection with known variance σ^2 of the object's position can be presented as the following formula [4]:

$$R_0^2 - R_1^2 \geq 2\sigma^2 \ln(\lambda_{cr}), \tag{1}$$

where $R_0^2 = \sum_{k=1}^{N_{mea}}((x_k - \hat{\bar{x}})^2 + (y_k - \hat{\bar{y}})^2)$ and $R_1^2 = \sum_{k=1}^{N_{mea}}\left((x_k - \hat{x}_k(\hat{\theta}_x))^2 + (y_k - \hat{y}_k(\hat{\theta}_y))^2\right)$ are residual sums of squared deviations of the object's position for verification of the hypotheses accordingly [26];

$x_k(\theta_x) = x_0 + V_x(\tau_k - \tau_0)$ and $y_k(\theta_y) = y_0 + V_y(\tau_k - \tau_0)$ are the estimations of positional coordinates of the object at τ_k time;

$\theta_x = (x_0, V_x)^T$, $\theta_y = (y_0, V_y)^T$ are the vectors of object's parameters along each coordinate;

x_0, y_0 are the positional coordinates of object at τ_0 time;
V_x, V_y are the velocities of object along coordinates *x* and *y*;
λ_{cr} is the threshold of a likelihood ratio.

2.2. Fisher f-criterion

In case when it is not possible and realistic to use the known variance of the object's position, authors suggested using the developed detection algorithm based on the Fisher *f*-criterion [27]. Using the *F*-test it is possible to check a statistical significance of the object's velocity along two axes (coordinates *x* and *y*). In such case a statistic of the *f*-distribution has no dependencies on the distribution of errors of the object's position [28].

Also, the Fisher distribution statistics has already predefined values from the table [26, 29]. The method for the object's NZAM detection based on the Fisher *f*-criterion can be presented as the following formula [22]:

$$\frac{R_0^2 - R_1^2}{R_1^2} \geq \frac{wf_{cr}}{N_{mea} - r}, \quad (2)$$

where *r* is the rank of a plan matrix F_x ($F_x = r \leq min(m, N_{mea})$) [26];

$w = 1$ is an amount of factors of a linear regression model (only apparent motion of object);

$m = 4$ is the number of estimated parameters of the object's motion along 2 axes: coordinates (x_0, y_0) at time τ_0 of base frame's timing and velocities (V_x, V_y) along each coordinate;

N_{mea} is a count of measurements of the investigated object from each image in series;

f_{cr} is a threshold of the Fisher distribution from the table [29].

According to the known count of measurements of the investigated object from each image in series N_{mea}, it is easy to determine the degrees of freedom for the f-distribution [29]. Also, the predefined significance level α helps to select the appropriate threshold of the f-distribution from the table.

3. Mathematical modeling

3.1. Number of experiments for mathematical modeling

In common case, the errors of experimental frequencies in the mathematical modeling are defined by estimates of CPFD γ_0 and CPTD γ_1. The acceptable values for them were predefined by authors, so $\gamma_{0accept} = \alpha/10$ and $\gamma_{1accept} = 10^{-3}$. Also, the dependence of the number of experiments and the errors of experimental frequencies in the mathematical modeling were defined by the following formulas: $N_{0exp} = 10^2 / \gamma_{0accept}$, $N_{1exp} = 10^2 / \gamma_{1accept} = 10^6$.

According to the research purposes only 10^3 of the smallest values of decisive statistics [30] were selected. Such data set also can be used for the Wavelet coherence analysis [31] as an alternative method of data analyzing.

3.2. Preconditions for mathematical modeling

To perform the mathematical modeling the following preconditions were defined:

- rectangular coordinate system (CS) with zero point *(0;0)* was used during the mathematical modeling;
- velocity module *V* is presented in the RMS error of measurement deviations of the position of object ($V = k\sigma$);
- object's apparent motion is uniform and linear, so the velocity module is $V = \sqrt{V_x^2 + V_y^2}$;
- modeling of the appropriate velocity module *V* is based on the angle γ, so the velocity projections are the following: $V_x = V sin\gamma$ and $V_y = V cos\gamma$;

- preliminary calibration sessions prepare the external variance σ_{out}^2, which is used as a known variance σ^2 of the object's position for the statistical and in situ modeling for method (1);
- modeling of the hypothesis H_0 ($V = 0$) provides a possibility to calculate a threshold λ_{cr} for the method (1) in accordance with the predefined significance level α;
- in accordance with the predefined significance level α and the appropriate degrees of freedom (1, 4), the threshold f_{cr} for the f-distribution in method (2) is also predefined and can be selected from the table [29].

3.3. Test data for in situ modeling

The appropriate test data for in situ modeling were selected in scope of the current research from the following real observatories: ISON-NM and ISON-Kislovodsk with unique observatory codes "H15" and "D00" accordingly. The information about these observatories is provided in the Table 1. The observatory codes are unique and approved by the Minor Planet Center (MPC) [32] of the International Astronomical Union (IAU) [33].

Table 1
Information about observatories

Observatory	Code	Telescope
ISON-Kislovodsk	D00	19.2-cm GENON telescope (VT-78) with wide field of view (FOW)
ISON-NM	H15	40-cm SANTEL telescope (400AN)

Test data for in situ modeling are consist of the different series of CCD-frames that were collected during the regular observations by the various CCD-cameras. The information about the CCD-cameras that are installed on the telescopes from the observatories list above is presented in the Table 1. This table contains the following information about CCD-camera: model and its parameters, like resolution, pixel size and exposure time.

Table 2
Information about CCD-cameras

Code	CCD-camera	Resolution	Pixel size	Exposure time
D00	FLI ML09000-65	4008 × 2672 pixels	9 microns	180 seconds
H15	FLI ML09000-65	3056 × 3056 pixels	12 microns	150 seconds

Each series of CCD-frames includes the different investigated objects in each frame of series. The main restriction during the test data preparation was selection only series of frames that contain the appropriate investigated object in each of them. The number of frames N_{img} in series was from four to eight. The average time between such frames was about ten minutes.

3.4. Random values for statistical modeling

The random values for the method of statistical modeling are normally distributed [34] and generated using the Ziggurat method [35]. This is a method for a sampling of the pseudo-random numbers. It belongs to the methods type for sampling rejection and its underlying source is related to the uniform distributed random numbers. Ziggurat method in general is a pseudo-random number generator, which uses the already predefined tables for randomization of numbers.

Ziggurat method generates the appropriate values that have a probability distribution, which always monotonically decreases. It can also be applied for the normal distribution as a symmetric unimodal distribution by selecting the value from one half of the distribution and then randomly selecting what part of the value will be drawn from. The common value created by the Ziggurat method requires only a generating of the one random float point and one random index of the table.

After this the appropriate table will be looked up with the further multiply operation and one comparison.

To generate the random value distributed by the normal law $N_x(m, \sigma^2)$ with mathematical expectation m and standard deviation σ, the randomized variable by the normal law $N_x(0, 1)$ should be multiplied with standard deviation σ and then added to the mathematical expectation m.

3.5. Constants for mathematical modeling

To perform the mathematical modeling the following constants were used for modeling:

- significance level (error of the 1st kind) $\alpha = (10^{-3}; 10^{-4})$;
- count N_{img} of frames of the investigated series $N_{img} = (4; 6; 8; 10; 15)$;
- velocity coefficient $k = (0; 0.5; 1; 1.25; 1.5; 1.75; 2; 3; 4; 5; 10)$;
- mean of the external estimation of RMS error of position $m(\sigma_{out}) = 0$;
- external estimation of RMS error of position $\sigma(\sigma_{out}) = (0.15; 0.25)$;
- angular direction of the object's apparent motion $\gamma = 45°$;
- thresholds of a f-distribution with ($1; 4$) freedom degrees are: $f_{cr} = 74.13$ $(\alpha = 10^{-3})$ and $f_{cr} = 241.62$ $(\alpha = 10^{-4})$ [29].

3.6. Mathematical modeling

Mathematical modeling for a NZAM detection of objects in the series of CCD-frames is described in the papers [3, 4]. But in general, a method for the mathematical modeling contains two major stages:

- modeling for the verification of a hypothesis H_0 when the investigated object has no apparent motion in both two directions in the image plane;
- modeling for the verification of an alternative hypothesis H_1 when the investigated object has at least 3σ-velocity or more.

Each stage of modeling for verification of both hypotheses has the common sequence of actions:

- determining of the experiment parameters;
- modeling of the appropriate number of experiments including the OLS-evaluation of the object's motion parameters;
- determining of both final values of the likelihood ratio of the methods (1) and (2);
- determining of both thresholds of the likelihood ratio and the f-distribution according to the appropriate significance levels;
- comparing of both final values of the likelihood ratio of the methods (1) and (2) with the appropriate thresholds that were calculated during modeling of the hypothesis H_0;
- determining of the CPTD: $D_{true} = N_{exc} / N_{1exp}$, where N_{exc} is an amount of exceeding of critical values.

The described above algorithm for the mathematical modeling is presented in the Figure 1 in view of the UML-diagram. According to the described in section 3.1. number of experiments for mathematical modeling the following common sequence of actions is performed for each k-th experiment (Figure 2):

- formation the set of positional measurements of objects with a NZAM;
- adding the appropriate deviations using random generator for each positional measurement of objects for modeling the hypothesis H_0;
- adding the appropriate velocity for each positional measurement of objects for modeling the hypothesis H_1;
- performing the OLS-evaluation of the object's motion parameters;
- performing the interpolation of the objects coordinate's estimation;

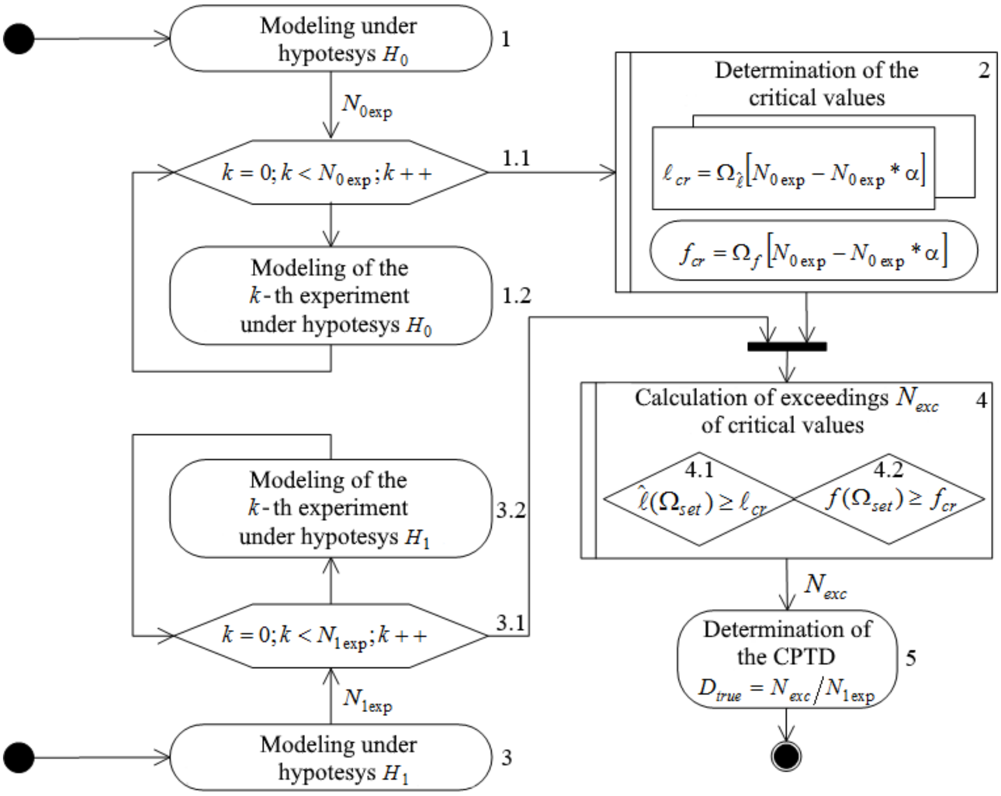

Figure 1: Algorithm for the mathematical modeling in view of the UML-diagram

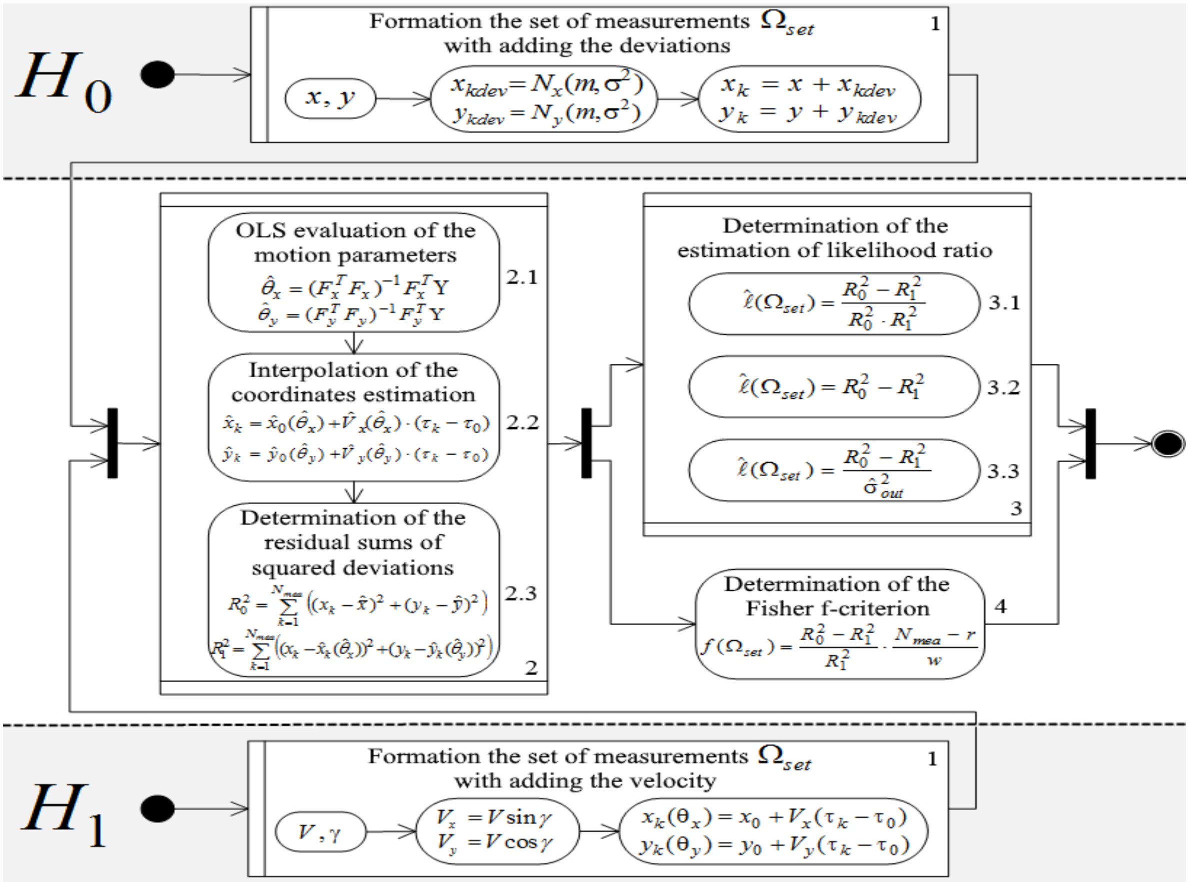

Figure 2: Common sequence of actions for each k-th experiment of the mathematical modeling in view of the UML-diagram

- determination of the residual sums of squared deviations;
- determination of the estimation of the appropriate likelihood ratio according to the selected detection method (1);
- determination of the Fisher f-criterion for the method (2);

The described above common sequence of actions for each *k*-th experiment of the mathematical modeling is presented in the Figure 1 in view of the UML-diagram.

4. Modeling results analysis

According to the calculated CPTD of the object's NZAM, the detection curves for the methods (1) and (2) were created as a proof of efficiency of the selected detection algorithms. Such detection curves were plotted using the basic calculations according to the modeling method and the received calculated information in view of CPTD. Such information is provided below in the following sections of this paper.

4.1. Statistical modeling

The processing results in terms of the CPTD after statistical modeling stage during mathematical modeling are presented in the Table 3. This table contains the following information: count of frames N_{img}, significance level α, list of the different values of generated apparent velocity in the RMS error of measurement deviations of the position of object ($V = k\sigma$), where the coefficient k was taken according to the definition above.

Table 3
Processing results after statistical modeling stage during mathematical modeling

Method	Count of frames $N_{img} = 4$, significance level $\alpha = 10^{-4}$								
	0	0.5σ	σ	1.25σ	1.5σ	1.75σ	2σ	3σ	4σ
1	0.0001	0.0002	0.0007	0.0011	0.002	0.003	0.005	0.03	0.109
2	0.0003	0.0005	0.0025	0.0043	0.007	0.01	0.016	0.06	0.147
Method	Count of frames $N_{img} = 8$, significance level $\alpha = 10^{-4}$								
	0	0.5σ	σ	1.25σ	1.5σ	1.75σ	2σ	3σ	4σ
1	0.0001	0.0017	0.0248	0.0679	0.152	0.285	0.456	0.939	0.999
2	0.0004	0.0697	0.7416	0.9555	0.996	0.999	1	1	1
Method	Count of frames $N_{img} = 15$, significance level $\alpha = 10^{-4}$								
	0	0.5σ	σ	1.25σ	1.5σ	1.75σ	2σ	3σ	4σ
1	0.0001	0.0767	0.8261	0.9842	0.999	1	1	1	1
2	0.0005	0.93	1	1	1	1	1	1	1
Method	Count of frames $N_{img} = 4$, significance level $\alpha = 10^{-3}$								
	0	0.5σ	σ	1.25σ	1.5σ	1.75σ	2σ	3σ	4σ
1	0.001	0.0027	0.0118	0.0234	0.043	0.065	0.123	0.475	0.852
2	0.0024	0.006	0.021	0.0348	0.057	0.076	0.125	0.353	0.635
Method	Count of frames $N_{img} = 8$, significance level $\alpha = 10^{-3}$								
	0	0.5σ	σ	1.25σ	1.5σ	1.75σ	2σ	3σ	4σ
1	0.001	0.1267	0.8625	0.9873	0.999	1	1	1	1
2	0.0037	0.7176	0.96	1	1	1	1	1	1
Method	Count of frames $N_{img} = 15$, significance level $\alpha = 10^{-3}$								
	0	0.5σ	σ	1.25σ	1.5σ	1.75σ	2σ	3σ	4σ
1	0.001	0.8157	0.98	1	1	1	1	1	1
2	0.004	0.93	1	1	1	1	1	1	1

According to the data received after processing and applying the statistical modeling stage during mathematical modeling from the Table 3, the detection curves for the methods (1) and (2) were created.

The Figure 3 shows the detection curves for objects with a NZAM for the method (1) with variance $\sigma_{out} = 0.25$ (dotted line) and the method (2) (solid line) after the statistical modeling stage during mathematical modeling.

The x-axis is a velocity V of the apparent motion of objects with a NZAM and the y-axis is a CPTD D_{true}.

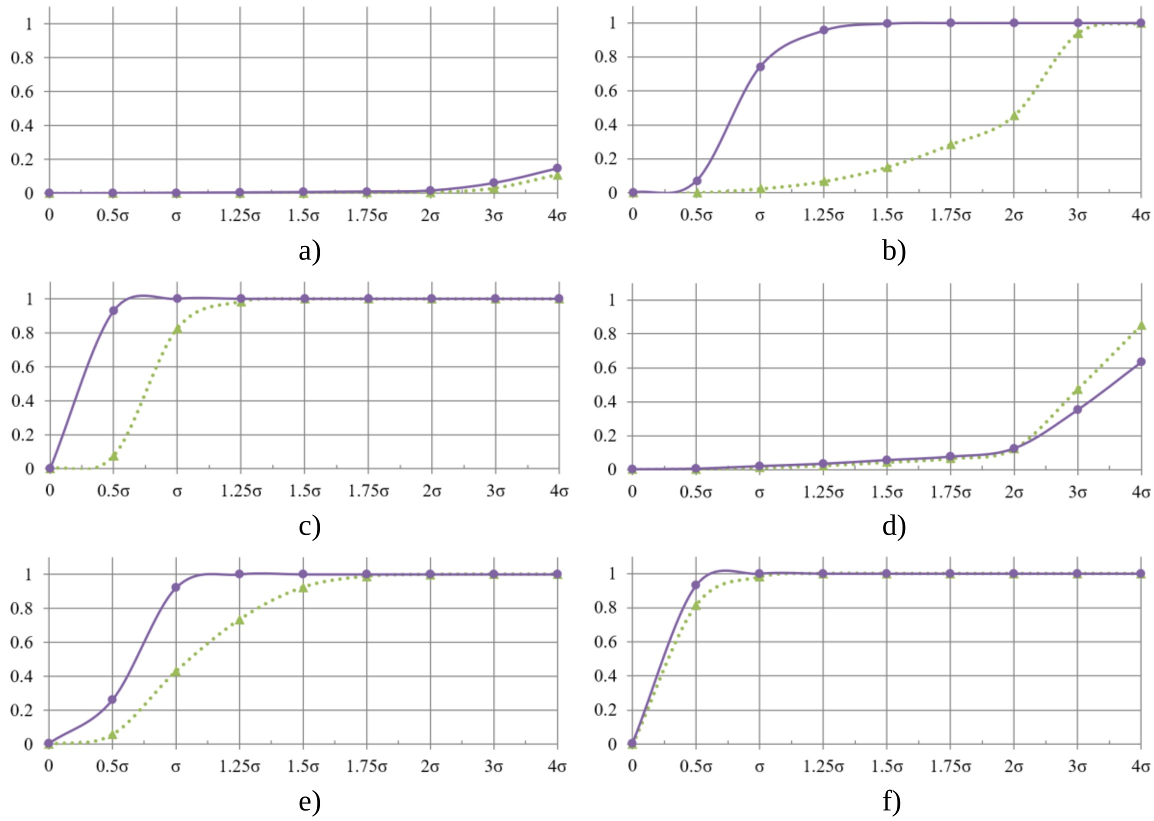

Figure 3: Detection curves after the statistical modeling stage during mathematical modeling for the objects with a NZAM for: a) $N_{img} = 4$ and $\alpha = 10^{-4}$; b) $N_{img} = 8$ and $\alpha = 10^{-4}$; c) $N_{img} = 15$ and $\alpha = 10^{-4}$; d) $N_{img} = 4$ and $\alpha = 10^{-3}$; e) $N_{img} = 8$ and $\alpha = 10^{-3}$; f) $N_{img} = 15$ and $\alpha = 10^{-3}$.

4.2. In situ modeling

During the in situ modeling stage of the mathematical modeling as a precondition step the RMS error of position σ_{out} of objects in series of CCD-frames was determined from the previous calculations as an instrumental error of the telescopes, which were used under research. The RMS error of position σ_{out} is presented in the Table 4 for each used telescope.

Also, the total number of all investigated objects N_{obj} with nullable motion is presented for the appropriate telescopes in the same table below.

Table 4
Information about telescopes and in situ modeling parameters

Telescope	Code	σ_{out}	N_{obj}
19.2-cm GENON telescope (VT-78) with wide field of view (FOW)	D00	0.33485	509906
40-cm SANTEL telescope (400AN)	H15	0.18624	114720

The processing results in terms of the CPTD after in situ modeling stage during mathematical modeling are presented in the Table 5. This table contains the following information: count of frames N_{img}, significance level α, list of the different values of generated apparent velocity in the RMS error of measurement deviations of the position of object ($V = k\sigma$), where the coefficient k was taken according to the definition above.

The main point of the in situ modeling is that the objects with no apparent motion (fixed objects) were taken from the prepared internal catalogue (IC) with fixed objects in all CCD-frames of the investigated series.

Table 5

Processing results after in situ modeling stage during mathematical modeling

Method	H15, significance level $\alpha = 10^{-4}$										
	0	0.5σ	σ	1.25σ	1.5σ	1.75σ	2σ	3σ	4σ	5σ	10σ
1	0.001	0.001	0.003	0.004	0.005	0.007	0.012	0.03	0.05	0.25	1
2	0.002	0.031	0.141	0.208	0.271	0.332	0.385	0.54	0.63	0.69	0.87
Method	H15, significance level $\alpha = 10^{-3}$										
	0	0.5σ	σ	1.25σ	1.5σ	1.75σ	2σ	3σ	4σ	5σ	10σ
1	0.001	0.001	0.001	0.002	0.003	0.005	0.007	0.05	0.41	0.93	1
2	0.002	0.127	0.356	0.441	0.506	0.559	0.602	0.72	0.79	0.84	0.96
Method	D00, significance level $\alpha = 10^{-4}$										
	0	0.5σ	σ	1.25σ	1.5σ	1.75σ	2σ	3σ	4σ	5σ	10σ
1	0.001	0.003	0.004	0.005	0.006	0.012	0.062	0.28	0.9	0.99	1
2	0.004	0.147	0.242	0.281	0.316	0.349	0.379	0.48	0.57	0.64	0.86
Method	D00, significance level $\alpha = 10^{-3}$										
	0	0.5σ	σ	1.25σ	1.5σ	1.75σ	2σ	3σ	4σ	5σ	10σ
1	0.001	0.002	0.007	0.013	0.023	0.044	0.139	0.84	0.98	0.99	1
2	0.003	0.231	0.360	0.413	0.460	0.503	0.542	0.67	0.76	0.83	0.98

According to the data received after processing and applying the in situ modeling stage during mathematical modeling from the Table 5, the detection curves for the methods (1) and (2) were created.

The Figure 4 shows the detection curves for objects with a NZAM for the method (1) with variance $\sigma_{out} = 0.25$ (dotted line) and the method (2) (solid line) after the in situ modeling stage during mathematical modeling.

The x-axis is a velocity V of the apparent motion of objects with a NZAM and the y-axis is a CPTD D_{true}.

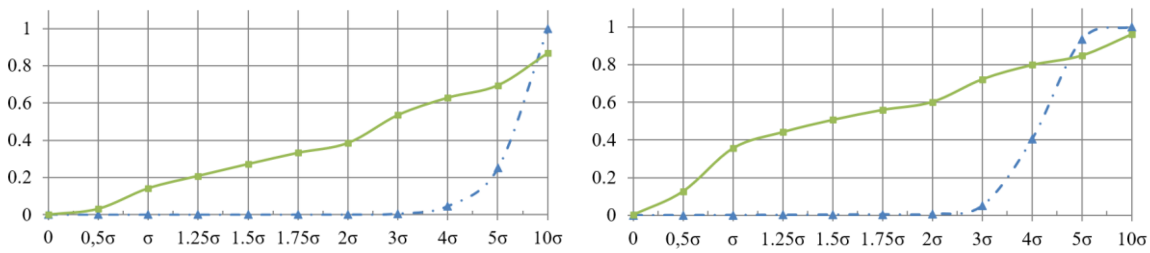

a) b)

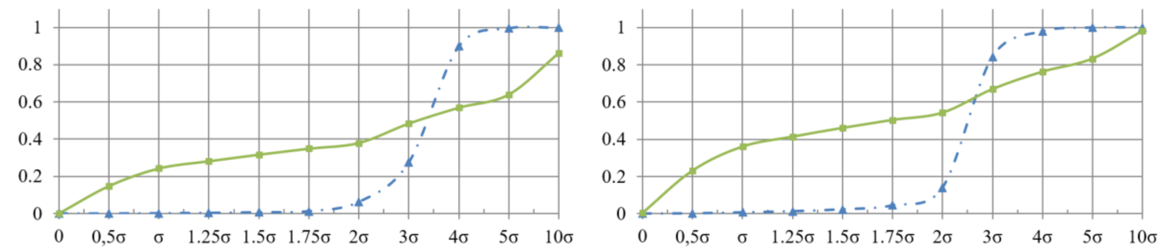

c) d)

Figure 4: Detection curves after the in situ modeling stage during mathematical modeling for the objects with a NZAM for: a) H15 and $\alpha = 10^{-4}$; b) H15 and $\alpha = 10^{-4}$; c) D00 and $\alpha = 10^{-4}$; d) D00 and $\alpha = 10^{-3}$.

4.3. Comparison

Regarding the statistical modeling stage during mathematical modeling the analysis shows that the method (1) with external variance $\sigma_{out} = 0.25$ is more delicate to changes in the object's apparent motion (see Figure 3 b) and e)).

Also, the method (2) is not so good when the number of frames N_{img} in series is small. But if it is not less than $N_{img} = 8$, this method is more effective by CPTD than other detection algorithms [4] (see Figure 3 b), c), e) and f)).

Regarding the in situ modeling stage during mathematical modeling the research shows that the method (1) with variance $\sigma_{out} = 0.25$ is not very effective when the object's velocity is less than $V = 3\sigma$ (see Figure 4 a) and c)).

But at the same time the method (2) is more delicate to changes in the object's apparent motion (see Figure 4 b) and d)).

4.4. Implementation

The architecture of an information system consists of the following main components: telescope -> software for saving the raw data -> server for the data collecting -> developed method for mathematical modeling (Figure 1) -> main detection algorithms -> accuracy indicators analysis.

A method for the mathematical modeling for a NZAM of objects in a series of CCD-frames was developed using the C++ programming language. A few general C++ methods are presented below:

- generating the appropriate deviations using random generator for each positional measurement of objects for modeling the hypothesis H_0 (Figure 5);
- performing the OLS-evaluation of the object's motion parameters (Figure 6);
- modeling of the hypothesis H_0 (Figure 7);
- modeling of the hypothesis H_1 (Figure 8).

```
double error()
{
    double sum = 0;
    for (int i = 0; i < 12; i++)
    {
        double x = (double)rand() / RAND_MAX;
        sum += x;
    }
    sum -= 6;
    sum *= sko;
    sum += expectedValue;

    return sum;
}
```

Figure 5: Generating the appropriate deviations using random generator

```
void getMotionParameters(double *empiricX, double *empiricY, double *t,
                        double &startX, double &startY, double &Vx, double &Vy)
{
    double Ax = 0, Bx = 0, Ay = 0, By = 0, C = 0, D = 0;

    for (int i = 0; i < N; i++)
    {
        Ax += empiricX[i];
        Bx += (t[i] - t[0]) * empiricX[i];

        Ay += empiricY[i];
        By += (t[i] - t[0]) * empiricY[i];

        C += (t[i] - t[0]);
        D += (t[i] - t[0]) * (t[i] - t[0]);
    }

    startX = (D * Ax - C * Bx) / (D * N - C * C);
    Vx = (Bx * N - C * Ax) / (D * N - C * C);

    startY = (D * Ay - C * By) / (D * N - C * C);
    Vy = (By * N - C * Ay) / (D * N - C * C);
}
```

Figure 6: OLS-evaluation of the object's motion parameters

```
void getCriteriaForH0()
{
    criteriaForH0.clear();
    for (int i = 0; i < numberOfExperiments; i++)
    {
        double empiricX[N], empiricY[N], t[N];
        for (int j = 0; j < N; j++)
        {
            t[j] = timeBetweenFrames * j;
            empiricX[j] = error();
            empiricY[j] = error();
        }

        double x[N], y[N];
        getSmoothCoordinates(empiricX, empiricY, t, x, y);

        double R0 = 0, R1 = 0;
        getResidualSumOfSquares(empiricX, empiricY, t, x, y, R0, R1);

        double MNKLymXY = 0;
        if (abs(R0) > eps) MNKLymXY = (R1 - R0) * (N * 2 - 4) / R0;

        criteriaForH0.push_back(MNKLymXY);
    }

    sort(criteriaForH0.begin(), criteriaForH0.end());

    int i = numberOfExperiments * alfa;
    threshold = criteriaForH0[numberOfExperiments - i];
}
```

Figure 7: Modeling of the hypothesis H_0

```
void getCriteriaForH1(double x0, double y0, double V)
{
    int cnt1 = 0;
    for (int i = 0; i < numberOfExperiments; i++)
    {
        double Vx, Vy;
        getSpeed(V, Vx, Vy);
        double empiricX[N], empiricY[N], t[N];
        for (int j = 0; j < N; j++)
        {
            t[j] = timeBetweenFrames * j;
            empiricX[j] = x0 + t[j] * Vx + error();
            empiricY[j] = y0 + t[j] * Vy + error();
        }

        double x[N], y[N];
        getSmoothCoordinates(empiricX, empiricY, t, x, y);

        double R0 = 0, R1 = 0;
        getResidualSumOfSquares(empiricX, empiricY, t, x, y, R0, R1);

        double MNKLymXY = 0;
        if (abs(R0) > eps) MNKLymXY = (R1 - R0) * (N * 2 - 4) / R0;
        if (MNKLymXY - threshold > eps) cnt1++;
    }

    printf("%.5f\n", 1.0 * cnt1 / numberOfExperiments);
}
```

Figure 8: Modeling of the hypothesis H_1

5. Conclusions

We developed a method for the mathematical modeling for a NZAM of objects of objects in a series of CCD-frames. The methods for statistical [1, 4] and in situ modeling [3] were also developed and used in scope of the mathematical modeling. Such method helps to evaluate the accuracy of computer vision [18] in scope of the NZAM detection of astronomical objects.

The especial variables and preconditions for the mathematical modeling were defined as well as their clarification. The method with a maximum likelihood criterion (1) [36, 37] and the method with Fisher distribution (2) [22, 38] we selected as the detection algorithms for a NZAM of objects for our research.

A method for the mathematical modeling for a NZAM of objects in a series of CCD-frames was developed using the C++ programming language (Figures 5-8). The modeling results were analyzed using the especial quality indicator (CPTD).

The obtained results from the Tables 3, 5 and Figures 3, 4 showed that the method (2) for the object's NZAM detection based on the Fisher *f*-criterion is more delicate to changes in the object's apparent motion and is very effective when the object's velocity is less than $V = 3\sigma$. The CPTD is up to 95 percent and only depends on the variance values. Such results were confirmed by both modeling types statistical and in situ.

The received results after processing by the developed method including the generated experiments with statistical and in situ data will be also used for the Wavelet coherence analysis [39, 40].

6. Acknowledgements

The authors thank all observatories, online services and tools that provided data to conduct the current research for testing the developed method.

7. References

[1] V. Shvedun, S. Khlamov, Statistical modelling for determination of perspective number of advertising legislation violations, Actual Problems of Economics 184 (2016) 389–396.

[2] T. Ando, Bayesian model selection and statistical modeling, CRC Press, 2010.

[3] M. Zhao, L. Huang, R. Zeng, et al., In-situ observations and modeling of metadynamic recrystallization in 300M steel, Materials Characterization 159 (2020) 109997. doi: 10.1016/j.matchar.2019.109997.

[4] W. Wu, F. Guo, J. Zheng, Analysis of Galileo signal-in-space range error and positioning performance during 2015–2018. Satell Navig 1 (2020), 1–13. doi: 10.1186/s43020-019-0005-1.

[5] A. Tantsiura, et al., Evaluation of the potential accuracy of correlation extreme navigation systems of low-altitude mobile robots, International Journal of Advanced Trends in Computer Science and Engineering 8 (2019) 2161–2166. doi: 10.30534/ijatcse/2019/47852019.

[6] M. Ivanov, et al., Effective informational entropy reduction in multi-robot systems based on real-time TVS, in: Proceedings of the IEEE International Symposium on Industrial Electronics, ISIE'19, Vancouver Canada, 2019, pp. 1162–1167, 2019. doi: 10.1109/ISIE.2019.8781209.

[7] X. Zhou, et al., Swarm of micro flying robots in the wild, Science Robotics, vol. 7, issue 66, eabm5954, 2022. doi: 10.1126/scirobotics.abm5954.

[8] V. Akhmetov, et al., Cloud computing analysis of Indian ASAT test on March 27, 2019, in: Proceedings of the IEEE International Scientific-Practical Conference: Problems of Infocommunications Science and Technology, PIC S&T'19, Kyiv Ukraine, 2019, pp. 315–318. doi: 10.1109/PICST47496.2019.9061243.

[9] S. Khlamov, et al., Data Mining of the Astronomical Images by the CoLiTec Software, CEUR Workshop Proceedings 3171 (2022) 1043–1055.

[10] G. E. Smith, The invention and early history of the CCD, Rev. Mod. Phys 3 (2010) 2307–2312.

[11] S. Khlamov, et al., Recognition of the astronomical images using the Sobel filter, in: Proceedings of the International Conference on Systems, Signals, and Image Processing, IWSSIP'22, Sofia Bulgaria, 2022, 4 p. doi: 10.1109/IWSSIP55020.2022.9854425.

[12] W. Burger, and M. Burge, Principles of digital image processing: fundamental techniques, Springer, New York, NY, 2009.

[13] Q. F. Zhang, et al. A comparison of centring algorithms in the astrometry of Cassini imaging science subsystem images and Anthe's astrometric reduction, Monthly Notices of the Royal Astronomical Society 505 (2021) 5253-5259. doi: 10.1093/mnras/stab1626.

[14] R. Gonzalez, R. Woods, Digital image processing, 4th edition, Pearson, New York, NY, 2018.

[15] A. M. Price-Whelan, et al., The Astropy Project: sustaining and growing a community-oriented open-source project and the latest major release (v5. 0) of the core package, The Astrophysical Journal 935 (2022) 167. doi: 10.3847/1538-4357/ac7c74.

[16] V. Savanevych, et al., CoLiTecVS software for the automated reduction of photometric observations in CCD-frames, Astronomy and Computing, vol. 40 (100605), 15 p., 2022. doi: 10.1016/j.ascom.2022.100605.

[17] S. Khlamov, and V. Savanevych, Big astronomical datasets and discovery of new celestial bodies in the Solar System in automated mode by the CoLiTec software, Knowledge Discovery in Big Data from Astronomy and Earth Observation, Part IV, Chapter 18, Astrogeoinformatics: Elsevier, pp. 331–345, 2020. doi: 10.1016/B978-0-12-819154-5.00030-8.

[18] V. Akhmetov, S. Khlamov, I. Tabakova, W. Hernandez, J. I. N. Hipolito, and P. Fedorov, New approach for pixelization of big astronomical data for machine vision purpose, in: Proceedings of the IEEE International Symposium on Industrial Electronics, ISIE'19, Vancouver Canada, 2019, pp. 1706–1710. doi: 10.1109/ISIE.2019.8781270.

[19] E.-J. Wagenmakers, and R. D. Morey, Simple relation between one–sided and two–sided Bayesian point–null hypothesis tests, Unpublished Manuscript, University of Amsterdam, 2013.

[20] E. L. Lehmann, J. P. Romano, and G. Casella, Testing statistical hypotheses, vol. 3, Springer, New York, NY, 2005.

[21] I. J. Myung, Tutorial on maximum likelihood estimation, Journal of mathematical Psychology 47 (2003) 90–100.

[22] B. Yazici, and M. Cavus, A comparative study of computation approaches of the generalized F-test, Journal of Applied Statistics 48 (2021) 2906–2919. doi: 10.1080/02664763.2021.1939660.
[23] M. E. J. Masson, A tutorial on a practical Bayesian alternative to null-hypothesis significance testing, Behavior research methods 43 (2011) 679–690. doi: 10.3758/s13428-011-0126-4.
[24] M. D. Lee, and E.-J. Wagenmakers, Bayesian cognitive modeling: A practical course, Cambridge University Press, 284 p., 2014.
[25] R. D., Morey and E.-J. Wagenmakers, Simple relation between Bayesian order-restricted and point-null hypothesis tests, Statistics & Probability Letters 92 (2014) 121–124. doi: 10.1016/j.spl.2014.05.010.
[26] R. Burden, J. Faires, and A. Reynolds, Numerical Analysis, Brooks/Cole: Boston, Mass: USA, 2010.
[27] L. Chai, L. Kong, S. Li, and W. Yi, The multiple model multi-Bernoulli filter based track-before-detect using a likelihood based adaptive birth distribution, Signal Processing 171 (2020) 107501. doi: 10.1016/j.sigpro.2020.107501.
[28] C. Ley, G. Reinert, and Y. Swan, Stein’s method for comparison of univariate distributions, Probability Surveys 14 (2017) 1–52. doi: 10.1214/16-PS278.
[29] G. Mélard, On the accuracy of statistical procedures in Microsoft Excel 2010, Computational statistics 29 (2014) 1095–1128. doi: 10.1007/s00180-014-0482-5.
[30] S. Y. Park, and A. K. Bera, Maximum entropy autoregressive conditional heteroskedasticity model, Journal of Econometrics 150 (2009) 219-230. doi: 10.1016/j.jeconom.2008.12.014.
[31] M. Dadkhah, et al., Methodology of wavelet analysis in research of dynamics of phishing attacks, International Journal of Advanced Intelligence Paradigms 12 (2019) 220–238. doi: 10.1504/IJAIP.2019.098561.
[32] The Minor Planet Center (MPC) of the International Astronomical Union. URL: https://minorplanetcenter.net.
[33] List Of Observatory Codes: IAU Minor Planet Center. URL: https://minorplanetcenter.net/iau/lists/ObsCodesF.html.
[34] N. Samuel, and M. Fernando, Can we rely on random number generators in statistical software?, Volume VII, 2018.
[35] G. Marsaglia, and W. Tsang, The ziggurat method for generating random variables, Journal of Statistical Software 5 (2000) 1–7. doi: 10.18637/jss.v005.i08.
[36] W. Qing, et al., Fast Inspect And Locate UKF Pipeline Leakage Based on Maximum Likelihood Criterion, in: Proceedings of the 5th IEEE Information Technology, Networking, Electronic and Automation Control Conference, volume 5 of ITNEC’21, 2021, pp. 697–700. doi: 10.1109/ITNEC52019.2021.9586974.
[37] L. Mykhailova, et al., Method of maximum likelihood estimation of compact group objects location on CCD-frame, Eastern-European Journal of Enterprise Technologies 5 (2014) 16–22. doi:10.15587/1729-4061.2014.28028.
[38] S. C. Gupta, V. K. Kapoor, Fundamentals of mathematical statistics, Sultan Chand & Sons, 2020.
[39] D. Kirikkaleli, J. K. Sowah, A wavelet coherence analysis: nexus between urbanization and environmental sustainability, Environmental Science and Pollution Research 27 (2020) 30295-30305. doi: 10.1007/s11356-020-09305-y.
[40] Z. Zhou, et al., Assessing the responses of vegetation to meteorological drought and its influencing factors with partial wavelet coherence analysis, Journal of Environmental Management 311 (2022) 114879. doi: 10.1016/j.jenvman.2022.114879.